

# FA-MA203 Research Internship – Report

Student: J. J. (Julian) Bosch, BSc

Daily supervisor: Dr. M.Y.M. (Rifka) Peeters

Referee: Prof. dr. C.A.J. (Catherijne) Knibbe

Examiner: Dr. M.P.H. (Marcel) van den Broek



Department of Clinical Pharmacy, St. Antonius Hospital, Utrecht, the Netherlands.



**Utrecht  
University**

Department of Pharmaceutical Sciences, Utrecht University, Utrecht, The Netherlands.

Date: June 28, 2023

# Population pharmacokinetic modelling of carboplatin in preterm and term neonates and young infants: towards dose individualization

## Abstract

**Background and objective:** Carboplatin has a place in the treatment of retinoblastoma and neuroblastoma in neonates and young infants. A typical treatment cycle consists of three consecutive days of treatment every three weeks, with the first day involving a dose that is based on body weight (BW). Current carboplatin dosing often involves therapeutic drug monitoring (TDM) to achieve the desired target exposure. The objective of this study is to develop a population pharmacokinetic (PK) model which accounts for relevant demographic covariates, that, in the end, allows for dose individualization of carboplatin in both preterm and full-term neonates and young infants.

**Methods:** A dataset including TDM data and patient characteristics, among which variables such as body weight at birth (BWB) and gestational age (GA), of 94 patients was obtained from the United Kingdom (UK). With the included patients, population PK modelling and systematic covariate analysis were performed using NONMEM. The developed model was used for dosing regimen evaluation and optimization.

**Results:** 67 patients with a median GA of 40 weeks (29.0-42.1 weeks, 8 with a preterm GA and 57 with a full-term GA), a median body weight at birth (BWB) of 3.26 kg (0.700-4.65 kg) and a median postnatal age (PNA) of 43.0 days (1.00-183 days) when starting their first carboplatin treatment cycle were included. BW was identified as the most important covariate for  $Cl$  and  $V_2$  in a two-compartment model, explaining 23.3% and 25.3% of the interindividual variability in  $Cl$  and  $V_2$ , respectively. Based on the simulations a dose increase from 4.4 mg/kg BW to 5.6 mg/kg BW was proposed.

**Conclusions:** As BW emerged as the most important covariate for carboplatin exposure, it seems justified to continue dosing based on BW. The simulations implied the need for a higher initial dose, so increasing the initial dose to 5.6 mg/kg BW while still employing TDM needs to be considered. Subsequently, TDM might gradually be phased out in the term infant group. Precaution should be taken when dosing carboplatin in preterm patients, as the model seemed to fit their data less well.

**Keywords:** neonates; young infants; carboplatin; pharmacokinetics.

## Introduction

Optimal dosing of anti-tumor drugs in neonates and young infants represents a major clinical challenge (annex 1). Drug disposition can change significantly during the first weeks of life due to a range of physiological changes (Veal et al., 2015). Furthermore, the maturation process during the prenatal period plays a crucial role in the subsequent changes observed in drug disposition during the early weeks of life. These changes can have a major impact on exposure and thus efficacy and toxicity. As both maximum efficacy and minimal toxicity are desirable, finding the right dose is a challenge of foremost importance. Individualized dosing has the

potential to lead to better outcomes in this challenging age group.

Carboplatin is a second-generation platinum-based drug that has a place in the first line therapy of some types of infant cancers, including retinoblastoma and neuroblastoma (Nijstad et al., 2022). It acts by forming inter- and intrastranded crosslinks in deoxyribonucleic acid (DNA) and hereby it induces cell cycle arrest followed by apoptosis of the affected cell. The treatment cycle of retinoblastoma or neuroblastoma involves three consecutive days of treatment every three weeks. The efficacy in afore mentioned indications has been well proved. Drug-related adverse reactions include nephrotoxicity, ototoxicity, neurotoxicity and

myelosuppression (Zhang, Xu, Gao, & Yao, 2022). Both adult and pediatric studies are consensual in the conclusion that exposure to carboplatin, measured as the area under the plasma drug concentration-time curve (AUC) of free carboplatin, strongly correlates with toxicity and response. Moreover, it has already been known for a while that cumulative AUC more closely correlates with toxicity and response than the dose administered does (Jodrell et al., 1992) (Newell et al., 1993). Allen et al. demonstrated that young patients (median age 8.6 months) receiving a dose based on body surface area (BSA), were 3.0 times more likely to have a platelet transfusion than their AUC based dose receiving counterparts (Allen et al., 2010). Thus, measuring exposure seems to be beneficial. For distinct types of tumors different target exposures have therefore been drawn up. Over a cumulative period of three days the target AUC varies from 5,2 mg/mL\*min in neonates with retinoblastoma to 21 mg/mL\*min in adults with medulloblastoma (Barnett, Kong, Makin, & Veal, 2021).

Marked physiological changes in the first weeks after birth are seen in both preterm and term neonates (Veal et al., 2015). Ontogeny describes the development of the physiology from the very beginning until obtaining a physiological function comparable to that of an adult (Veal & Boddy, 2012). Development of blood flow, the kidneys and hepatic enzymes can all influence the pharmacology of drugs. However, the rate of development can differ within the group of newborns. For instance, there is some recent compelling evidence that suggests that neonates and young infants with a higher gestational age (GA) show an overall faster maturation of glomerular filtration rate (GFR) with increasing postnatal age (PNA) than their lower GA peers (Wu et al., 2022). Also, the baseline value can differ. The nephrogenesis starts at approximately five weeks of gestation and is completed by approximately 36 weeks. As a result, preterm neonates have a lower GFR than term neonates. GFR can be as low as 0,6-0,8 mL/min/1,73 m<sup>2</sup> in preterm neonates whilst values of 2-4 mL/min/1,73 m<sup>2</sup> are usual in term neonates (Veal & Boddy, 2012). At birth GFR seems to be determined by body weight at birth (BWB), thereafter the maturation rate of GFR is dependent on GA and PNA (Wu et al., 2022).

Since carboplatin clearance from the body occurs almost exclusively via renal filtration of unchanged drug, renal function has an undeniable impact on pharmacokinetic

(PK) values, including AUC (Veal et al., 2015). Knowing one's GFR will help predict carboplatin exposure in that particular individual. Estimating GFR is a well-established practice in adult populations. Various validated methods can be used, with both endogenous and exogenous markers belonging to the (Rodieux, Wilbaux, van den Anker, & Pfister, 2015). However, these methods may be less suitable to use for the neonatal population. On the one hand, the most commonly used endogenous marker creatinine reflects maternal levels in the first weeks of life because the placenta allows free transfer of creatinine between the mother and her unborn infant. Moreover, creatinine undergoes passive reabsorption in the renal tubule in early infancy. On the other hand, measurement of GFR markers, such as inulin, iohexol, 51Cr-EDTA or 99mTc-diethylenetriaminepenta-acetic acid is difficult in pediatric patients due to ethical and practical reasons.

Therefore, current practice of carboplatin dosing in neonates and young infants generally comprises therapeutic drug monitoring (TDM), in order to achieve the target AUC and with that, reduce toxicity and improve response. Recent investigation in all 21 pediatric oncology centers in the United Kingdom (UK) showed that TDM was used in the majority of patients (Roberts, Mogg, Barnfield, & Veal, 2020). The initial dose is commonly based on body weight (BW), as BSA is less useful in this population because it tends to cause overdosing more often (Nijstad et al., 2022). However, dosing on BW is not ideal either. Veal, Errington et al. have reported that nearly all preterm and full-term neonates and young infants with an initial dose based on BW need a dose adjustment based on the results of TDM (Veal et al., 2015). Both underdosing and overdosing were seen.

This calls for a PK model that allows for dose individualization on the following grounds: (1) to be able to immediately target the first dose within therapeutic range and; (2) to be less TDM dependent. With no models focusing on specifically carboplatin in neonates and young infants being published, it is not clear which covariates and which functions best predict the observed heterogenous pattern of carboplatin exposure in this population. The objective of our study is to develop a population PK model which accounts for relevant demographic covariates, that, in the end, allows for dose individualization of carboplatin in both preterm and full-term neonates and young infants.

# Materials and methods

## Dataset, ethical approval and privacy measures

In 2019, a TDM dataset of 27 neonates and young infants from the UK with retinoblastoma or low risk neuroblastoma receiving carboplatin was obtained from Gareth J Veal, professor of Cancer Pharmacology at Newcastle University. In these patients, TDM was carried out with the purpose of dose optimization, complying with the latest guidelines on carboplatin in infants of the Children's Cancer and Leukaemia Group from the UK. For this reason, no ethical approval was needed for sample collection. Since the data set used in the our study was coded in the treating hospital and did not permit access to personal data during the analysis phase, there was no need to implement additional privacy measures. Veal GJ, as the primary investigator, was requested to provide an update incorporating new data, taking into account the significant time that has passed since the acquisition of the previously mentioned data. The data was requested to be provided in the same format. As of May 2023, TDM data from 94 subjects were obtained.

Since our study retrospectively analyzed data collected for the purpose of the standard of care, it was not subject to the *Wet medisch-wetenschappelijk onderzoek met mensen* (WMO). The study was conducted in line with good clinical practice (GCP) and the AVG regulation.

## Blood sampling and analysis

The neonates and young infants receiving carboplatin were generally subjected to treatment on day one, two and three of a course of 21 days. Data were obtained from as many days as possible. However, plasma samples were not always obtained on each of the three days of treatment, with samples from day three missing most frequently. An explanation for this was that TDM was conducted to optimize the dose for the following day, aiming to reach the desired three-day target AUC. This optimization strategy made blood sampling on day three unnecessary.

Carboplatin was administered intravenously with an infusion duration of approximately one hour. Blood samples were collected at approximately half an hour after the start of the infusion, five minutes after the infusion ended, and approximately one hour after the

infusion ended. On some occasions, a fourth blood sample was taken. Accidentally, only two samples were obtained in total. All samples were taken from a different lumen to that used for carboplatin administration (Veal et al., 2010). Accurate recording of the precise sampling times was diligently maintained for each participant, and these recorded times were utilized for subsequent PK analysis.

To isolate plasma for free carboplatin concentration quantification, immediate centrifugation (1,200g, 4°C, 10 minutes) was employed to separate 2 mL whole blood samples into plasma and cellular components (Veal et al., 2010) (Veal et al., 2015). Subsequently, 1 mL of the obtained plasma was further processed using an Amicon Centrifree Micropartition unit with a 30,000 MW cut-off (Millipore, Edinburgh, UK). The plasma samples underwent an additional centrifugation step (1,500g, 4°C, 15 minutes) to yield plasma ultrafiltrate, which was specifically utilized for the determination of free carboplatin levels. The resulting plasma ultrafiltrate was promptly frozen at -20°C prior to subsequent analysis. All frozen samples were dispatched to the Northern Institute for Cancer Research, Newcastle University, via an overnight courier service. The samples were securely packaged in an insulated container with dry ice, maintaining a frozen state throughout transportation. Upon arrival at the laboratory, the samples were directly stored at -20°C until the time of analysis. It was confirmed that all samples arrived at Newcastle within 24 hours of dispatch from the clinical center, and their frozen state was maintained during transit.

Platinum sample analyses were carried out by flameless atomic absorption spectrophotometry (AAS) using a Perkin-Elmer AAnalyst 600 graphite furnace spectrometer (Perkin-Elmer Ltd, Beaconsfield, UK). The levels were determined in the previously described plasma ultrafiltrates. All samples were subject to duplicate analysis, and the reported values represent the average of these measurements. Duplicate values were within 15% in all cases. To ensure assay validity, the intra- and inter-assay coefficients of variation for a quality assurance sample had to be below 10%. The lower limit of detection for the assay was established at 0.10 lg/ml.

## Demographic data

Along with TDM data, other demographic information about the subjects was obtained. This included information on GA, PNA, PMA, BW, BWB, BSA and being

preterm or full-term at birth. Further relevant information such as the dose given, the infusion time and rate and the cumulative target AUC over three days was also collected. Exclusion criteria encompassed a missing GA, PNA, BW or BWB and a PNA of more than one year.

## Pharmacokinetic analysis

The development of a population PK model was constructed using non-linear mixed effects modelling (NONMEM) version 7.4.3. The parameter estimates of the models were obtained using subroutines ADVAN1 and TRANS2 for one compartment modelling and ADVAN6 and TOL5 for two compartment modelling. RStudio 2022.12.0 was used for tidying the dataset. Pirana 2.9.9 and RStudio 2022.12.0 were used for data visualization, by means of covariance tables, Goodness-of-fit (GOF) plots and individual plots with population predicted values (PRED), individual predicted values (iPRED), time after dose (TAD), observed values (DV) and conditional weighted residuals (CWRES) on the axes.

Firstly, an appropriate structural and statistical model with both inter- and intraindividual variability was built and then covariates were added to this basic model to establish any relationship with population parameters. To construct a structural model, the data set was partitioned into multiple subsets. Initially, an analysis was conducted on a subset consisting solely of the first day of the first cycle. Subsequently, a separate analysis was performed on a subset encompassing all days of the first cycle. Within these two subsets, potentially important covariates such as BW and PNA would exhibit minimal or no changes within a patient. This facilitated the development of a structural model. Several one- and two-compartment models were tested on the data, including the parameters clearance (Cl) and volume of distribution (V or V1), and in case of a two-compartment model also intercompartment clearance (Q) and peripheral volume of distribution (V2). The utilized basic parameters and functions to account for interindividual variability were as follows:

$$Cl = \theta(1) * \text{EXP}(\eta(1));$$

$$V1 = \theta(2) * \text{EXP}(\eta(2));$$

$$Q = \theta(3) * \text{EXP}(\eta(3));$$

$$V2 = \theta(4) * \text{EXP}(\eta(4));$$

where  $\theta$  (theta) is the typical value of the corresponding PK parameter in the population;  $\eta$  (eta) is a random

variable for an individual with a mean of zero and variance  $\omega^2$  (omega squared), assuming log normal distribution in the population. For residual variability an additive error model ( $Y = C_{\text{PRED}} + \epsilon_1$ ), a proportional error model ( $Y = C_{\text{PRED}} * (1 + \epsilon_1)$ ) and a combined error model ( $Y = C_{\text{PRED}} * (1 + \epsilon_1) + \epsilon_2$ ) were tested, where  $C_{\text{PRED}}$  is predicted carboplatin concentration for an individual and  $\epsilon$  (epsilon) a random variable with mean zero and variance  $\sigma^2$  (sigma squared). If Pirana data inspector showed correlation between two parameters, models were run in which these parameters were put in a so called  $\omega$ -block. Variation between cycles and within a cycle was explored by incorporating inter occasion variability (IOV) on the parameters by replacing  $(\eta(x))$  for  $(\eta(x) + \text{IOV})$ .

After the structural and statistical model was identified, covariates were plotted independently against the individual post hoc parameter estimates to identify their influence in the data subset of cycle 1. Tested covariates were: GA, BWB, BW, PNA and PMA. In case of an observed correlation, covariates were added to the PK parameters in a linear, linearly centered or allometric manner, in the dataset with all days of all cycles. In the functions,  $\theta(x)$  was substituted with one of the following partial functions, depending on the specific manner being utilized, corresponding to the aforementioned manners, respectively:

$$\theta(x) * \left( \frac{\text{COV}}{\text{median COV}} \right);$$

$$\theta(x) * (1 + \theta(y) * (\text{COV} - \text{median COV}));$$

$$\theta(x) * \left( \frac{\text{COV}}{\text{median COV}} \right)^{\theta(z)};$$

where  $\theta(x)$  is  $\theta(1)$ ,  $\theta(2)$ ,  $\theta(3)$  or  $\theta(4)$ ; COV is the covariate to be included in the model; median COV is the median value of the covariate for the population of the analyzed data set,  $\theta(y)$  represents the slope parameter for the linear covariate relationship and  $\theta(z)$  represents the exponent for a power function. When applying covariates in an allometric manner, the exponent was estimated rather than fixed. The objective of incorporating covariates was to account for the variability observed in the parameter. Therefore, an examination was conducted to determine if the inclusion of covariates led to a decrease in the  $\omega$  of the parameter. A successful estimation step indicated the ability to successfully estimate the parameter values.

Furthermore, the impact of the formula proposed by Wu et al. in 2021, which predicts GFR of both preterm and term neonates and young infants based on GA, BWB and PNA was tested on the clearance (literature review in appendix, paragraph 1.3.2) (Wu et al., 2022). Wu YJ was consulted to obtain an updated formula, which is expected to be published soon. The received formula

was subsequently tested as part of our study, referred to as formula Wu 2023. Both formulas were incorporated in the models by replacing  $\theta(1)$  for  $\theta(1) * GFR$ , where GFR represents the value calculated with the formula. In this way,  $\theta(1)$  represents the clearance expressed as a fraction of the estimated GFR.

$$\text{Formula Wu 2021: } GFR = CLp \cdot \left[ \frac{BWB}{1.75} + \left( \frac{GA}{34} \right)^a \cdot b \cdot \left( \frac{PNA}{2} \right)^{\left( \frac{GA}{34} \right)^c} \right]$$

$$\text{Formula Wu 2023: } GFR = 1.27 \cdot \left[ \frac{BWB}{1.75} + \left( 5.43 \cdot \left( \frac{BW}{1.75} \right)^{0.826} - \frac{BWB}{1.75} \right) \cdot \frac{PNA^{1.23}}{\left( 19 \cdot \left( \frac{GA}{34} \right)^{-3.64} \right)^{1.23} + PNA^{1.23}} \right]$$

*With:*

*GFR:* glomerular filtration rate in L/h in formula Wu 2021 and in mL/min in formula Wu 2023

*CLp:* 0.086 L/h

*a:* 9.99

*b:* 0.154

*c:* -1.71

*BWb:* birth weight in kilograms

*GA:* gestational age in weeks

*PNA:* postnatal age in days

## Statistical analysis

Choices concerning model structure and selection of covariates and the applied functions were based on three factors: (1) objective function value (OFV) and potential increase or decrease of OFV compared to a reference model, depicted by delta OFV (dOFV), with a dOFV lower than -7.8 indicating that the new model significantly better fits the data with a value of  $P < 0.005$ ; (2) parameter estimates and their calculated significance and; (3) GOF-plots including IPRED versus DV, PRED versus DV, PRED versus CWRES and DV versus CWRES. The GOF-plots were also analyzed separately for the different cycles. Furthermore, the confidence interval of the parameter estimates, the correlation matrix and

visual improvement of the individual plots were used to evaluate the model. Empirical Bayesian estimates of PK parameters were obtained from the final population model.

Potential covariates were individually included in the model. When multiple significant covariates with successful estimation steps were identified, the covariate that resulted in the largest decrease in the OFV was retained in the model. Additional covariates were required to further reduce the OFV by employing the same criteria in order to be included in the model. Additionally, the impact of including the covariate on the interindividual variability of the parameter was assessed. It was evaluated whether the interindividual variability of



the parameter was reduced upon inclusion of the covariate. The observations in the plots of  $\eta$  versus covariate were expected to exhibit random distribution around zero as part of the evaluation process.

The internal validity of the population PK model was assessed using the bootstrap resampling method, which involves repeatedly sampling from the original dataset to generate new datasets of the same size but with different combinations of individuals. In the bootstrap analysis, stratification based on the covariate preterm was performed to generate datasets that included a representative proportion of preterm neonates. The mean parameter values and confidence intervals (CI) of the bootstrap replicates were compared with the estimates of the original data set. Ideally, the model estimated parameters should always be within the 95% CI and it should not deviate with more than 20% from the median calculated with the bootstrap. A wide CI shows that a parameter is uncertain.

## Evaluation and optimization of dosing regimen

The current standard in carboplatin dosing was evaluated based on the developed model. Various dosing regimens were assessed to determine their efficacy in achieving comparable exposure among neonates and young infants with varying GA and PNA. Furthermore, the current standard in collecting carboplatin samples was evaluated in this study.

## Results

### Study population

A total of 67 patients were included in this study, based on the inclusion and exclusion criteria. The included patients started with carboplatin treatment between September 2006 and March 2023. Eight of the patients were born preterm (with GA ranging from 29 weeks to 35 weeks and 5 days), the other 59 were born term (with GA ranging from 37 weeks to 42 weeks and 1 day). At the commencement of carboplatin treatment, the age of the youngest patient included was one day, whereas the oldest patient included was 183 days old. For every individual between one and eight cycles were monitored (with a median of two). A treatment cycle comprised one or three days of active treatment, with a median duration of three days. The group receiving treatment just one day per cycle contained five patients. Among them, one patient switched to a three-day treatment regimen starting from the third cycle. The median number of days monitored per cycle of all patients was one. In total, 148 cycles were analyzed, comprising 173 doses and 491 blood samples. Patient characteristics and treatment characteristics are listed in table 1. Data about sex and the diagnosis for which treatment with carboplatin was initiated were not transmitted.

**Table 1.** Baseline characteristics of the included 67 (eight preterm and 59 term) neonates and young infants.

Parameter	Mean (SD)	Median (range)
<b>Patient characteristics</b>		
GA (weeks)	38.7 (2.69)	40.0 (29.0-42.1)
BWB (kg)	3.14 (0.793)	3.26 (0.700-4.65)
PNA on first day of first cycle (days)	60.9 (50.0)	43.0 (1.00-183)
PMA on first day of first cycle (weeks)	47.4 (7.39)	45.4 (29.1-65.9)
BW on first day of first cycle (kg)	4.41 (1.41)	4.30 (1.30-8.99)
PNA on first day of all cycles (days)	87.0 (62.7)	73.0 (1.00-294)
PNA per patient on first day of all cycles (days)	78.2 (53.2)	65.0 (1.00-218)
PMA on first day of all cycles (weeks)	51.3 (9.02)	49.6 (29.1-79.0)
PMA per patient on first day of all cycles (weeks)	49.9 (7.90)	49.8 (29.1-70.5)
BW on first day of all cycles (kg)	4.98 (1.59)	4.90 (1.30-9.00)

BW per patient on first day of all cycles (kg)	4.77 (1.48)	4.60 (1.30-8.99)
<b>Carboplatin treatment regimen</b>		
Duration treatment per cycle (days)	2.86 (0.510)	3.00 (1.00-3.00)
Dose on the monitored days (mg)	35.8 (26.6)	27.0 (4.50-200)
Dose per patient on the monitored days (mg)	35.3 (28.0)	26.0 (5.70-158)
Unit dose per kg BW on the monitored days (mg/kg)	6.97 (3.72)	6.14 (2.81-26.7)
Unit dose per kg BW on the first day of cycles of patients with three days of active treatment (mg/kg)	5.84 (1.68)	5.58 (3.30-10.6)
Duration infusion on the monitored days (min)	85.2 (31.3)	70.0 (51.0-180)
Infusion rate on the monitored days (mg/min)	0.464 (0.400)	0.317 (0.0882-2.90)
Target AUC of the monitored cycles (mg/mL*min)	6.06 (1.18)	5.20 (4.30-7.95)
Number of monitored cycles	2.21 (1.40)	2.00 (1.00-8.00)
Monitored days per cycle	1.17 (0.498)	1.00 (1.00-3.00)
Number of TDM samples per day	2.84 (0.556)	3.00 (1.00-5.00)

*Note: Where relevant, the characteristics displayed per patient represent the means of the mean per patient and the medians of the median per patient. SD: standard deviation. GA: gestational age. BWB: body weight at birth. PNA: postnatal age. PMA: postmenstrual age. BW: current body weight. TDM: therapeutic drug monitoring. AUC: area under the curve.*

## Model building

The concentrations of the 491 included carboplatin samples ranged from 0,69 µg/ml to 46,7 µg/ml, with sampling times varying from nineteen minutes to 370 minutes after the start of the infusion. All samples were included in the NONMEM analysis. The profile of the concentrations versus time is presented in figure 1.

### Structural model

Both a one-compartment and a two-compartment model were explored and optimized in order to determine the best fit for the data, as both models demonstrated a good description of the observed data. In the best one-compartment model, interindividual variability was incorporated for clearance and the volume of distribution. The best two-compartment model included interindividual variability for clearance, the volume of distribution of the central compartment, and the volume of distribution of the peripheral compartment, while assuming a fixed value of zero for the intercompartmental clearance (figure 2). The observed correlation between clearance and the volume

of distribution of the central compartment in Pirana Data Inspector prompted the implementation of a  $\omega$ -block on both parameters, leading to an improvement in the stability of the model. In both the best one-compartment and the best two-compartment model, a proportional error was found to provide the most accurate description of the residual variability. An additive error or a combined proportional and additive error model did not result in a significant better fit.

In both data subsets of cycle 1, the diagnostic plots and the parameter precision indicated that the two-compartment model provided the best fit for the observed data compared to the one-compartment model. In the subset containing all days of the first cycle, the number of significant digits in the final estimation was 3.8 and 3.4 for the two- and one-compartment model respectively. The diagnostic plots supported the superiority of the two-compartment model, as the scatter plot for the one-compartment model exhibited a banana-shaped pattern when examining the TAD versus the CWRES (figure 3). This pattern suggested the presence of a second compartment.



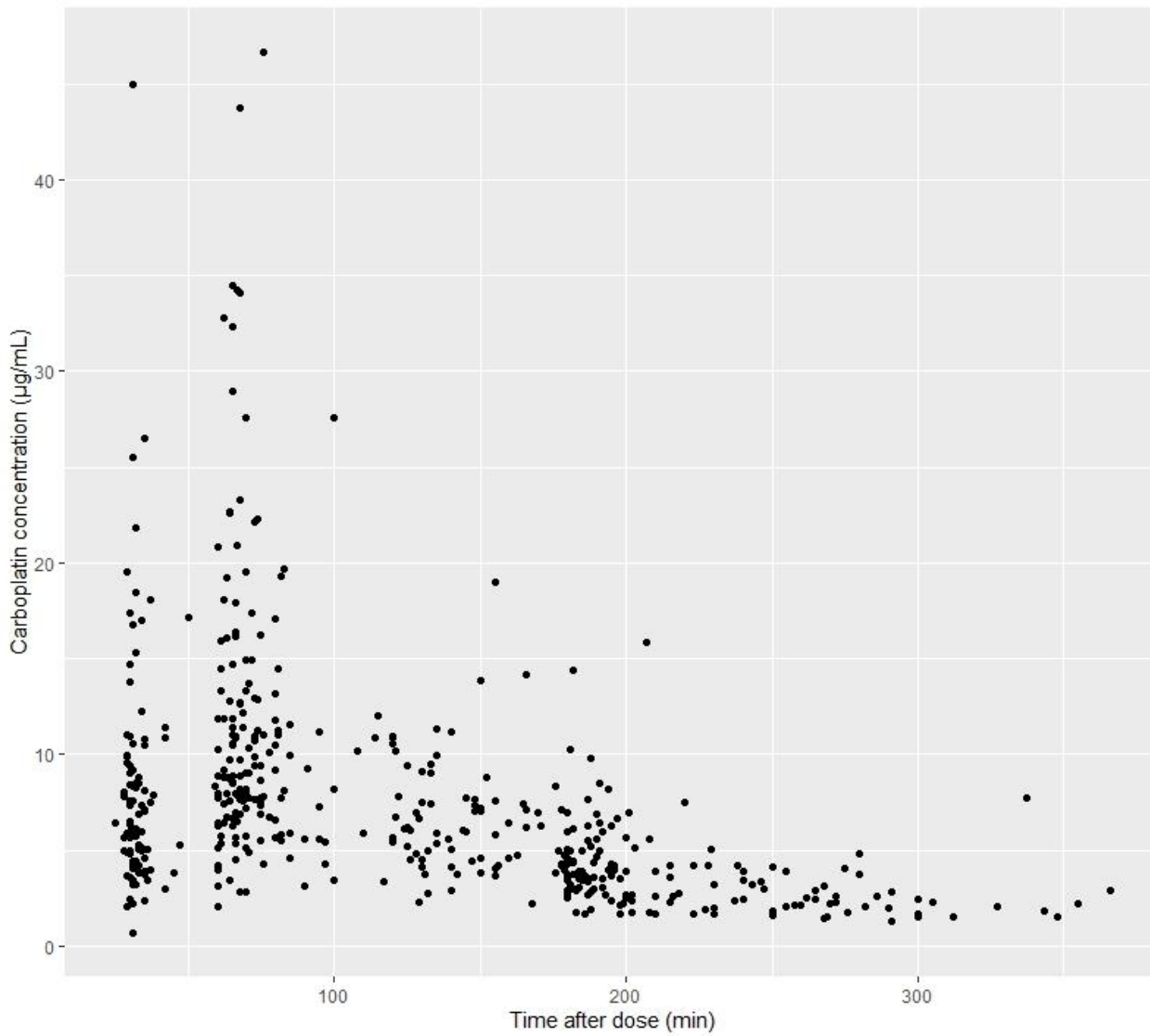


**Figure 1.** Observed carboplatin concentration (DV) versus time after the dose (TAD).

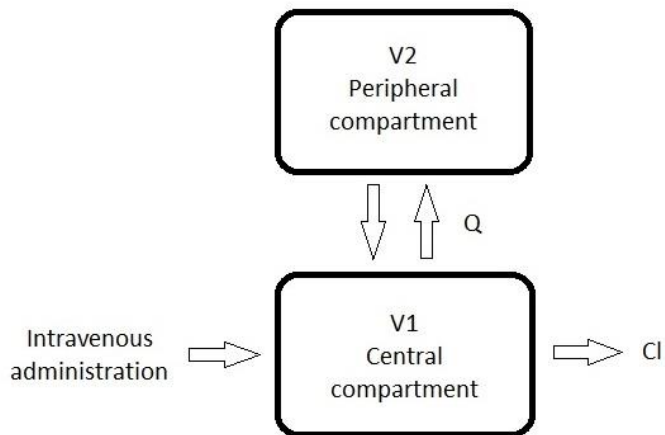


**Figure 2.** The best structural two-compartment pharmacokinetic model for carboplatin. V2: volume of distribution of the peripheral compartment. Q: intercompartmental clearance of carboplatin. Cl: elimination clearance.

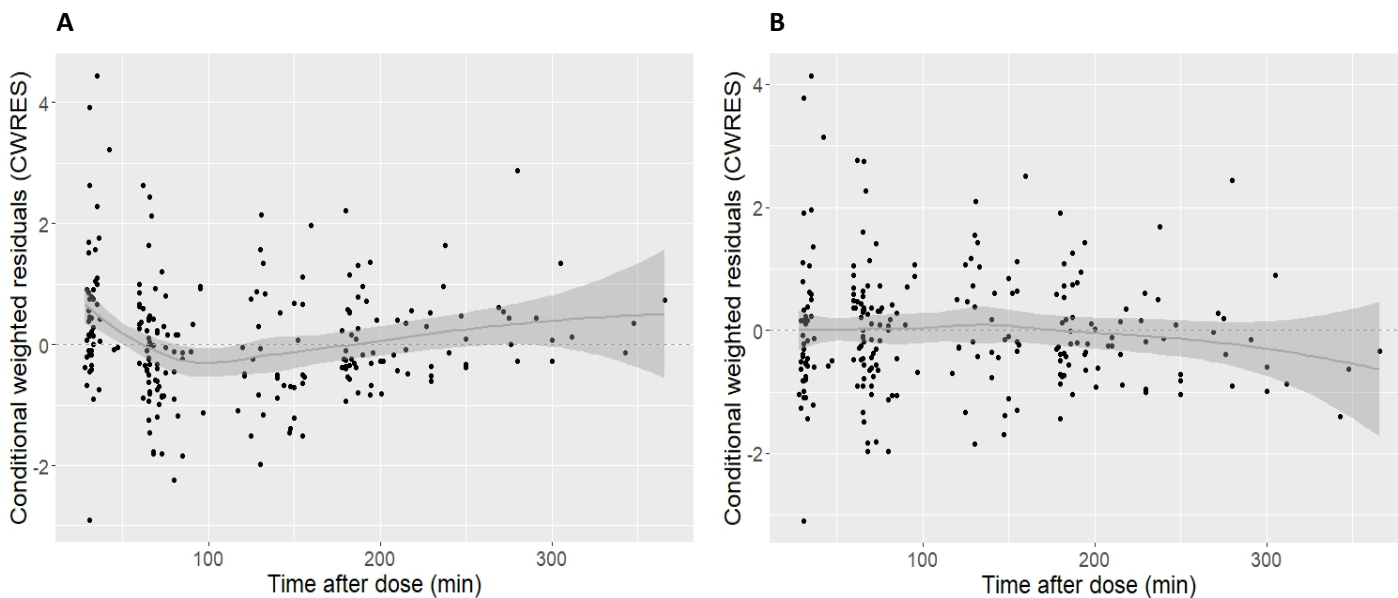


**Figure 3.** Time after dose (TAD) versus conditional weighted residuals (CWRES) of the best one-compartment model (A) and the best two compartment model (B) without covariates added to the pharmacokinetic (PK) parameters. The scatter plot for the one-compartment model exhibits a banana-shaped pattern, with early and late TAD showing more positive than negative CWRES.

### Covariate analysis

The majority of the single covariates exhibited a linear-like correlation with all PK parameters in the subset dataset of cycle 1. Therefore, all individual covariates were tested on all parameters in the full dataset, containing all days of all cycles. Despite the already observed linear-like correlations, all modeling approaches including the allometric method, were employed.

From the individual covariates, BW proved to be the most important covariate for CI (compared to PMA linearly centered,  $\Delta$ OFV of -137.616 units; PNA linearly centered,  $\Delta$ OFV of -111.958 units; GA linearly centered,  $\Delta$ OFV of -16.581 units) and caused a significant drop in OFV when applied linearly centered on the full data set ( $\Delta$ OFV of -177.442 units) (table 2). Furthermore, the

formula proposed by Wu et al. in 2021 and the updated formula from 2023 were incorporated in the clearance. This resulted in a drop in OFV of 114.75 and 169.383 respectively. Thus, the formula from 2023 proved to be superior to the formula of 2021 on  $\Delta$ OFV. However, it exhibited a smaller decrease of 7.754 units compared to BW ( $P < 0.05$ ).

BW emerged as the most significant covariate for V1 as well (compared to BWB linearly centered,  $\Delta$ OFV of -17.616 units) and caused a significant drop when applied allometric ( $\Delta$ OFV of -21.631 units). For V2, BW again proved to be the most important covariate (compared to PMA allometric,  $\Delta$ OFV of -92.679 units; PNA linearly centered,  $\Delta$ OFV of -89.388 units; BWB allometric,  $\Delta$ OFV of -11.435 units) and resulted in a significant decrease when implemented in an allometric manner ( $\Delta$ OFV of -130.116 units)

**Table 2.** Covariate analysis for the pharmacokinetic model of carboplatin in the dataset containing all days of all cycles.

PK parameter	Covariate	Approach	OFV	$\Delta$ OFV	Successful estimation step
Base model	-	-	1240.178	-	Yes
CI	BW	Linearly centered	1062.736	-177.442	Yes

		Allometric	1065.906	-174.272	Yes
	Wu 2023	Linear	1070.245	-169.383	Yes
	BW	Linear	1071.373	-168.806	Yes
	PMA	Linearly centered	1102.562	-137.616	Yes
		Allometric	1118.748	-121.43	Yes
	Wu 2021	Linear	1125.428	-114.75	No
	PNA	Allometric	1128.22	-111.958	No
		Linearly centered	1131.021	-109.157	Yes
	PMA	Linear	1152.023	-88.155	Yes
	PNA	Linear	1168.578	-71.6	No
	BWB	Linearly centered	1222.113	-18.065	No
		Allometric	1222.138	-18.04	No
		Linear	1222.138	-18.04	No
	GA	Linearly centered	1223.597	-16.581	Yes
		Allometric	125.043	-15.135	Yes
		Linear	1232.29	-7.888	Yes
V1	BW	Allometric	1218.547	-21.631	Yes
		Linearly centered	1219.627	-20.551	Yes
		Linear	1222.112	-18.066	No
	BWB	Linearly centered	1237.243	-17.616	Yes
	PMA	Allometric	1234.496	-5.682	Yes
		Linear	1234.88	-5.298	Yes
	PNA	Allometric	1235.437	-4.741	Yes
	PMA	Linearly centered	1235.523	-4.655	Yes
	PNA	Linearly centered	1237.088	-3.09	Yes
	GA	Linearly centered	1237.459	-2.719	Yes
		Allometric	1237.502	-2.676	No
		Linear	1237.784	-2.394	No
	BWB	Allometric	1237.791	-2.387	Yes
		Linear	1243.998	3.82	Yes
	PNA	Linear	1267.948	27.77	No
V2	BW	Allometric	1110.062	-130.116	Yes
	PMA	Allometric	1147.499	-92.679	Yes
	PNA	Linearly centered	1150.79	-89.388	Yes
		Allometric	1152.013	-88.165	No
		Linear	1152.997	-87.181	Yes
	BW	Linear	1161.861	-78.317	Yes
		Linearly centered	1167.031	-73.147	No
	PMA	Linearly centered	1194.772	-45.406	No
		Linear	1205.284	-34.894	Yes
	BWB	Allometric	1228.743	-11.435	Yes
		Linearly centered	1230.818	-9.36	No
		Linear	1231.976	-8.202	No
	GA	Linearly centered	1232.789	-7.389	Yes
		Allometric	1234.698	-5.48	Yes

Linear	1237.637	-2.541	Yes
--------	----------	--------	-----

Note: The first row represents the reference model, the two-compartment model with interindividual variability for Cl, V1 and V2, without added covariates, and with residual variability described by a proportional error. Cl: elimination clearance: V1: volume of distribution of the central compartment. V2: volume of distribution of the peripheral compartment. OFV: objective function value. ΔOFV: difference in OFV with the reference model. GA: gestational age. BWB: body weight at birth. BW: current body weight. PNA: postnatal age. PMA: postmenstrual age. Wu 2021 and Wu 2023: the formulas of Wu et al. from 2021 and 2023.

The model with BW linearly centered on Cl and BW linear on V2 and the model with Wu 2023 linear on Cl and BW linear on V2 were subsequently compared based on their estimates and their GOF plots. The number of significant digits in the estimates was identical in both models, with a value of 3.3. Among all the estimates, only the  $\omega$  of Cl in the Wu 2023 model had an RSE above 50%, specifically 66.8%. The GOF plots did not show a clear preference for any specific model. The subgroups with GA < 37 weeks and PNA < 14 days exhibited similar patterns in the GOF

plots of both models (paragraph Goodness-of-fit plots). As final PK model, the BW model was preferred over the Wu 2023 model, because of the significantly bigger decrease in OFV (14.244 units) and its simplicity. The final model can be found in annex 2. The parameter estimates of this final PK model are summarized and presented in table 3. The inclusion of BW resulted in a decrease in the interindividual variability of Cl from 40.4% to 17.1% and of V2 from 98.1% to 72.8%, a decrease of 23.3% and 25.3% respectively.

**Table 3.** Population pharmacokinetic parameters of the final covariate model and the results of the bootstrap analysis.

PK parameter	Full data set		Bootstrap analysis	
	Final estimate	RSE (%)	Sample median	Confidence interval (5 <sup>th</sup> to 95 <sup>th</sup> percentile)
Cl (mL/min) = $\theta_1 + \theta_2 * (BW - 4.90)$				
Value for $\theta_1$	15.7	3	15.6	14.7-16.7
Value for $\theta_2$	3.14	8	3.14	2.64-3.49
V1 (mL) = $\theta_3$				
Value for $\theta_3$	1020	11	1011	776-1193
Q (mL/min) = $\theta_4$				
Value for $\theta_4$	35.6	12	35.6	31.1-43.8
V2 (mL) = $\theta_5 * (BW/4.90)$				
Value for $\theta_5$	1370	14	1376	1112-1644
Interindividual variability				
Value for $\omega^2$ (Cl)	0.0287	31	0.0276	0.0139-0.0471
Value for $\omega^2$ (V1)	0.207	38	0.201	0.103-0.348
Value for $\omega^2$ (V2)	0.425	29	0.397	0.165-0.638

## Residual variability

Value for  $\sigma^2$

0.055

14

0.055

0.045-0.067

Note: the final model comprised two compartments with BW linearly centered on CI, with BW linear on V2 and with CI and V1 in a  $\omega$ -block. The bootstrap analysis was stratified on preterm patients and had 187 successful runs out of 250. PK: pharmacokinetic. RSE: relative standard error. CI: elimination clearance. V1: volume of distribution of the central compartment. Q: intercompartmental clearance of carboplatin. V2: volume of distribution of the peripheral compartment.  $\Theta$ : typical value in the population.  $\omega^2$ : interindividual variance.  $\sigma^2$ : proportional intraindividual variance.

## Goodness-of-fit plots

Model diagnostics of the final model were performed by analyzing the GOF results. As presented in figure 4A and B, the predictions of the patient group as a whole were largely unbiased. A slight bias was observed at higher

values in the plot of PRED versus DV (figure 4A). No trends were observed in the diagnostic plots of IPRED versus DV, PRED versus CWRES and TAD versus CWRES (figure 4B, C and D).

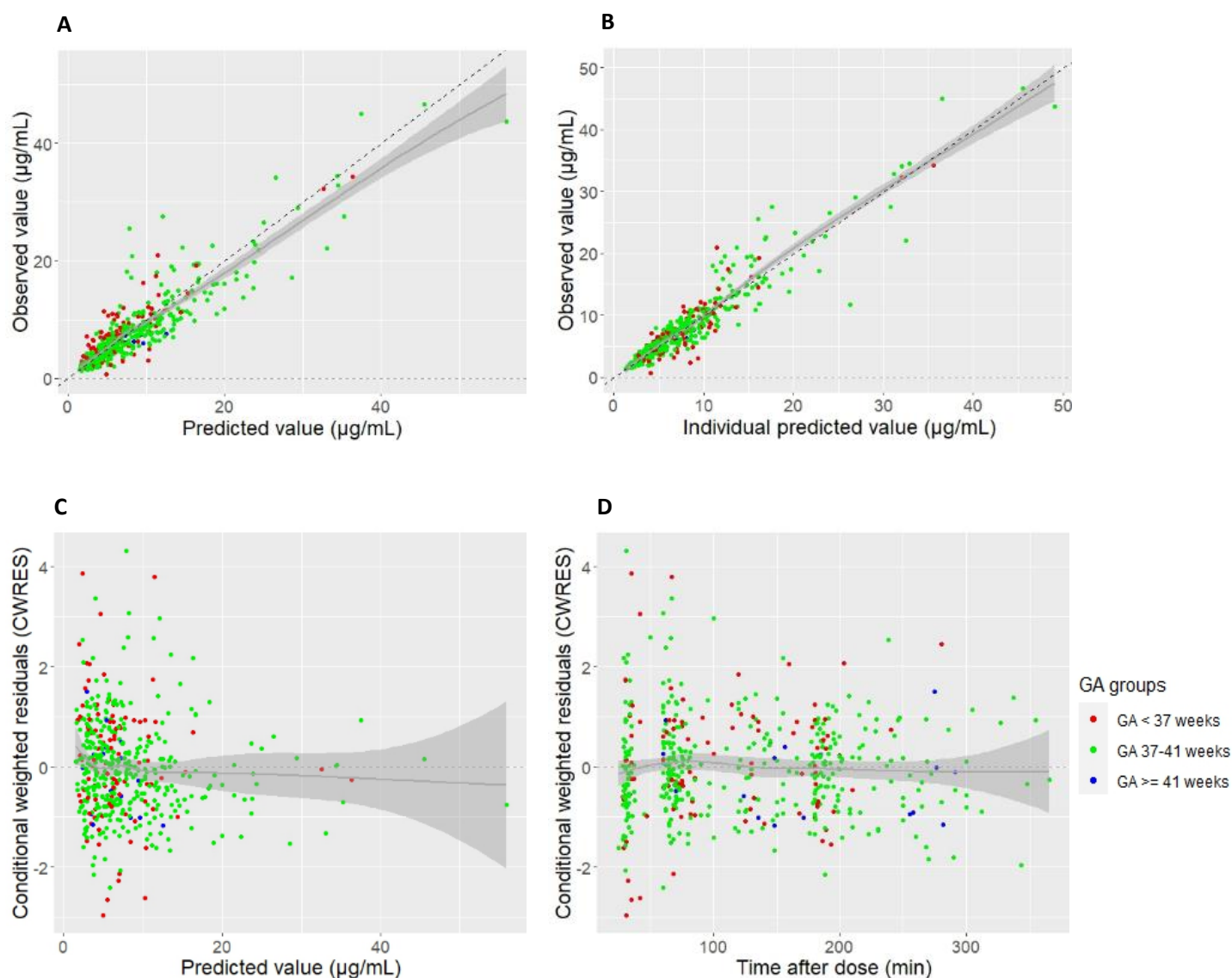
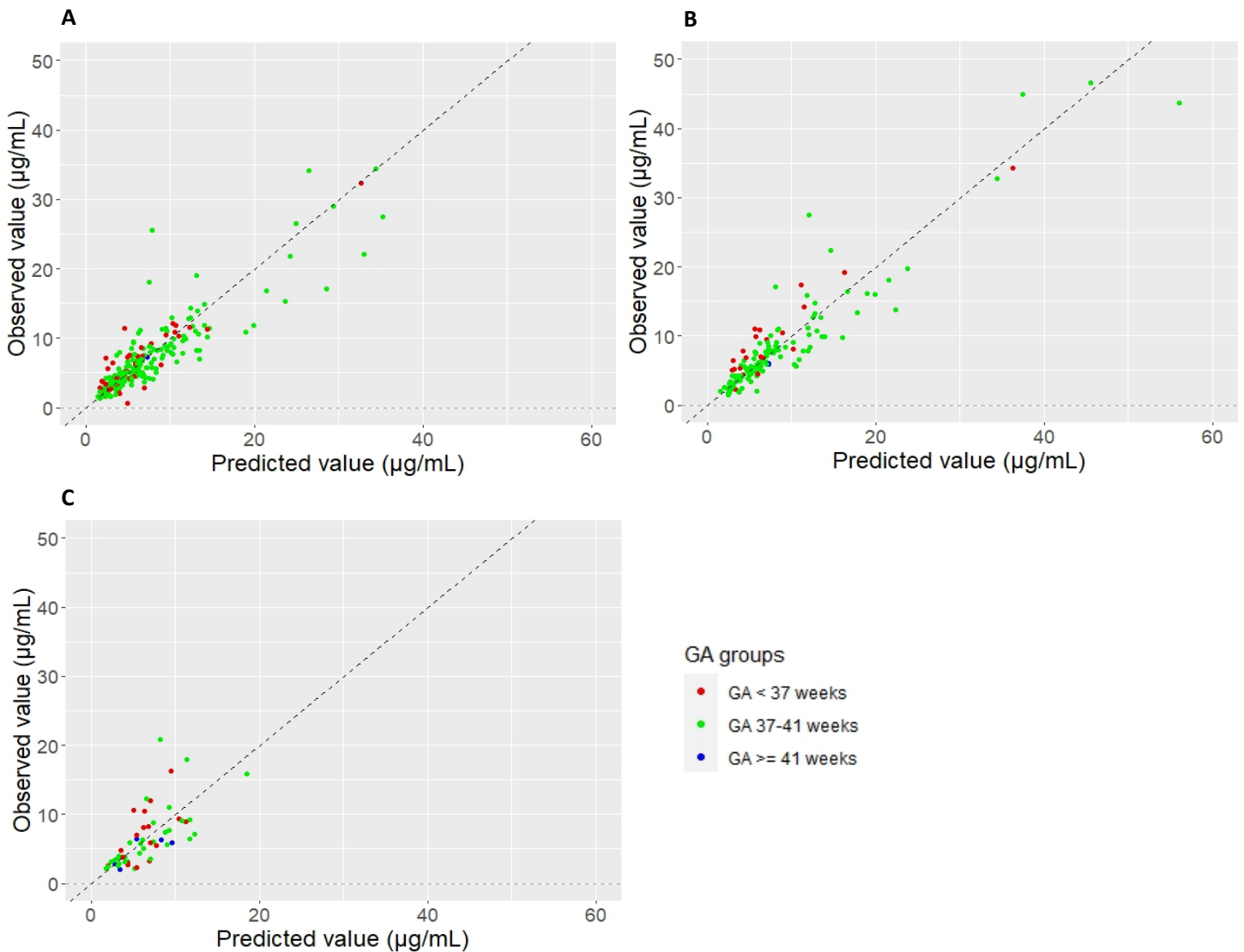


Figure 4. Goodness-of-fit results of the final model. (A) Population predicted value (PRED) versus observed value (DV). (B) Individual predicted value (IPRED) versus observed value (DV). (C) Population predicted value (PRED) versus conditional weighted residuals (CWRES). (D) Time after dose (TAD) versus conditional weighted residuals (CWRES). GA: gestational age.

When examining the different GA groups in the GOF plots, a subtle bias was noticeable in the plot of PRED versus DV, with patients with a GA lower than 37 weeks exhibited a trend of having higher DVs compared to PRED (figure 4A). Upon subdividing the data into different cycles, it was observed that the bias was primarily present in cycle 2 (figure 5). Further investigation was conducted by examining the plots of PRED versus CWRES and TAD versus CWRES specifically for cycle 2. Notably,

the bias was found to be unrelated to specific concentrations or sampling times.

Then, the GOF plots were reanalyzed, but this time for different PNA groups. The plot of PRED versus DV revealed a slight bias in patients with a PNA lower than 14 days, with a tendency toward lower DVs compared to PRED (figure 6). However, it should be noted that this bias arose from the data points of just two individuals.



**Figure 5.** Population predicted value (PRED) versus observed value (DV) for cycle one (A), cycle two (B) and cycle three (C). Cycles four to eight are not depicted because of the absence of data from preterm patients in those cycles. GA: gestational age.

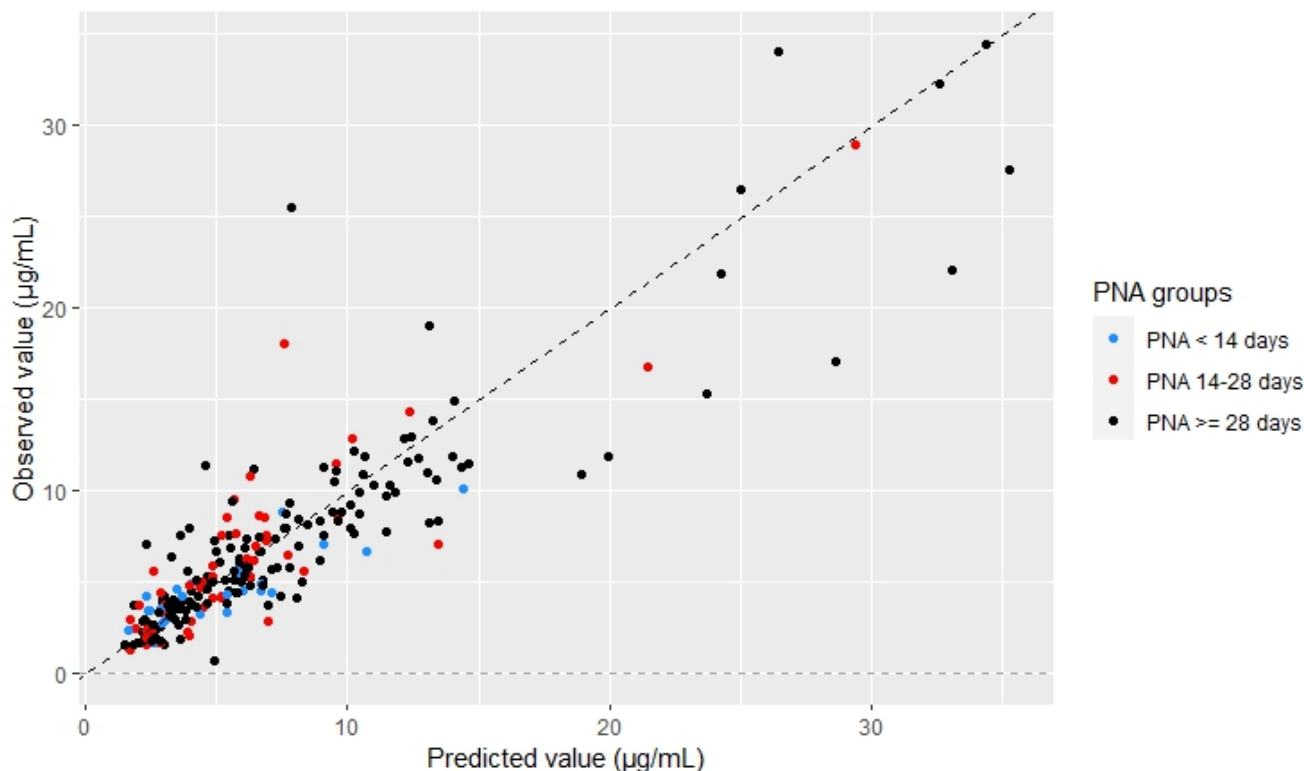


Figure 6. Population predicted value (PRED) versus observed value (DV) in cycle 1. PNA: postnatal age.

## Internal model validation

The bootstrap analysis, stratified on the covariate preterm, demonstrated the stability and reliability of the final model. The results are presented in table 3. Out of 250 runs, 63 runs were excluded when calculating the bootstrap results. 32 runs were terminated during the minimization process and 31 runs had estimates near a boundary. The parameter values calculated from the developed model with the remaining 187 runs were consistent with the median parameter estimates obtained from the bootstrap procedure. All bootstrapped medians showed a deviation of less than 20% from the final estimates, with the largest deviation observed at 7%.

## Dosing regimen evaluation and optimization

Four simulations were conducted using the final model, representing a preterm neonate, a term neonate, a preterm infant, and a term infant. The results of one of the hypothetical patients are presented in figure 7. The cumulative AUC over the three-day period was calculated assuming the standard dosing regimen of 4.4 mg/kg BW. The calculated AUC values were 3.93, 4.04,

4.08, and 4.13 mg/mL\*min for the preterm neonate, term neonate, preterm infant, and term infant, respectively.

To achieve a target AUC of 5.2 mg/mL\*min, the dose had to be increased in all simulated patients. The required doses to attain this target were found to be 5.80, 5.66, 5.60, and 5.54 mg/kg BW for the simulated preterm neonate, term neonate, preterm infant, and term infant, respectively. Thus, the findings from our final model suggested that the optimal daily dose for neonates and young infants was approximately 30% higher than the standard dosing regimen of 4.4 mg/kg BW.

The simulations also yielded valuable insights into the optimal sampling times. Based on the four simulated patients, it was found that approximately 50% of the daily AUC was achieved within 110-220 minutes after the start of the infusion, and 75% was reached within 240-420 minutes. In current practice, sampling is typically conducted up to two hours after the start of the infusion. However, to ensure that the last sample captures at least 50% of the AUC, it is recommended to extend the sampling period to four hours after the start of the infusion. This adjustment will help to obtain more accurate and representative measurements of carboplatin exposure.



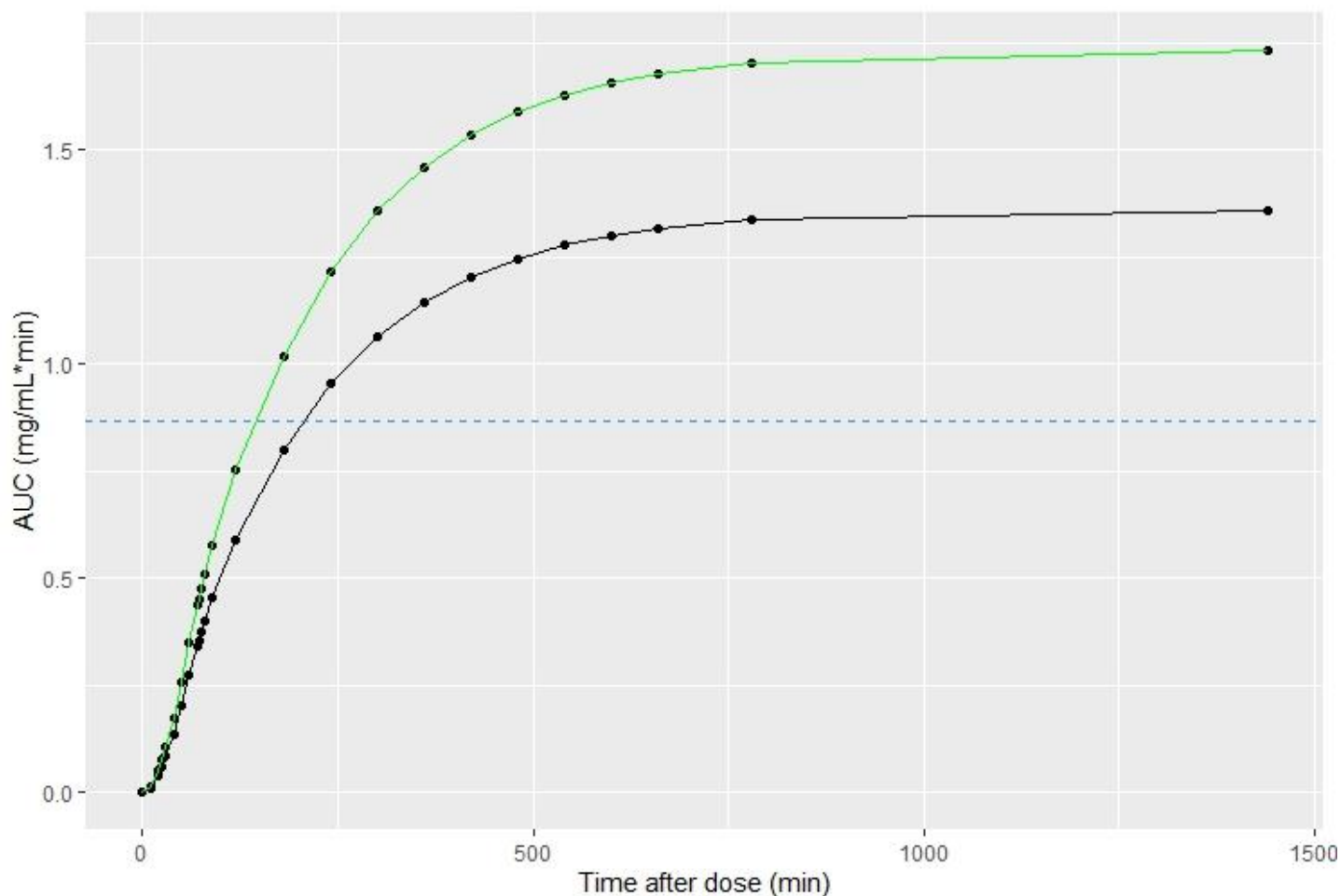


**Figure 7.** One-day simulation results of a hypothetical patient. The black curve represents the one-day AUC of carboplatin, assuming the standard dosing regimen of 4.4 mg/kg BW. The resulting one-day AUC is 1.46 mg/mL\*min. The green curve represents a dosing regimen which results in a one-day AUC of 1.73 mg/mL\*min (one third of the desired three-day AUC of 5.2 mg/mL\*min). The estimated dose required to achieve the green curve in this simulation is 5.6 mg/kg BW. The blue line corresponds to half of the target one-day AUC. In this hypothetical patient, this level is attained approximately 150 minutes after the start of the infusion, 90 minutes after its completion. AUC: area under the curve. BW: body weight.

## Discussion

The objective of this study was to develop the first population PK model for carboplatin in preterm and full-term neonates and young infants, accounting for relevant demographic covariates. The primary aim of this study was to enable better individualized dosing of carboplatin in this specific population. This research could have significant importance for pediatric centers involved in chemotherapy for neonates and young infants, as the current practice of using initial doses based on BW often requires subsequent dose adjustments based on TDM results. Our findings could help to be able to immediately target the first dose within therapeutic range and reduce the dependence on TDM for achieving the desired drug exposure. Moreover,

carboplatin is primarily eliminated renally, and estimating GFR in this subpopulation is challenging. Therefore, the development of a PK model incorporating only demographic covariates such as BW, BWB, GA, and PMA could significantly contribute to neonatology's understanding of renal development during the early stages of life. By elucidating the role of these covariates in carboplatin PK, our study offers valuable insights into renal function in neonates and young infants.

In this study, a population PK model for carboplatin was successfully developed using NONMEM, utilizing data from a total of 67 patients. The model employed a two-compartment structure with interindividual variability incorporated for V1, V2, and Cl, along with a proportional error to capture residual variability. The covariate

analysis revealed that BW emerged as the most important covariate for both CI and V2, with a  $\omega$ -block on CI and V1. Surprisingly, this final model exhibited a significantly greater reduction in the OFV compared to the model incorporating Wu et al.'s formula from 2023 for CI. This outcome was unexpected based on existing literature, which suggests substantial differences in renal function between preterm and term infants (Wu et al., 2022) (De Cock et al., 2012) (Guignard, 2017) (Rodieux et al., 2015) (Veal & Boddy, 2012). It was anticipated that Wu's formula, which predicts GFR based on GA, BWB, and PNA, would better capture renal function and yield a more pronounced OFV reduction in a population PK model of a renally cleared drug like carboplatin, as compared to BW alone. One possible explanation for the observed results is that the dataset used in this study may not have been sufficiently diverse to fully benefit from a formula that primarily distinguishes between preterm and term neonates. After all, our dataset contained only 8 preterm born patients out of a total of 67 patients. Furthermore, the median PNA of the first day of the monitored cycles of our dataset was 73 days, indicating a predominance of young infants rather than neonates, whilst neonates provided the basis of Wu's formula. Another factor to consider is that Wu's formula is still in preparation, so it is relatively new and has not yet undergone extensive validation. Therefore, at present, dosing based on BW remains the standard approach according to our population PK model. Simulations performed in NONMEM demonstrated that the optimal daily dose of carboplatin for neonates and young infants was approximately 30% higher than the currently recommended dosing regimen of 4.4 mg/kg BW. Based on these findings, neonates and young infants could receive an initial daily dose of about 5.6 mg/kg BW, provided blood levels are still being monitored in order to intervene in case of too high or too low exposure. Considering that the median unit dose on the first day of cycles in patients with three days of active treatment from your dataset was 5.58 mg/kg BW, it appears that the dose advice provided by the population PK model aligns with the standard practice observed in the dataset upon use of TDM to adjust the dose on day two and three. This further supports the validity of the model and suggests that the recommended dose of 5.6 mg/kg BW is consistent with the actual doses administered in clinical practice. Furthermore, based on the simulations, it was determined that extending the sampling period to four hours after the start of the infusion is necessary to

ensure that the last sample encompasses at least 50% of the daily AUC. This adjustment in the sampling schedule will enhance the accuracy of carboplatin exposure assessment and provide more reliable data for PK analysis. Ideally, it would be preferable to take samples when an even greater portion of the AUC has been attained. However, it is also important to maintain practical feasibility. Clinical centers should assess the feasibility of this extension, also considering the potential burden on the child.

Despite the overall unbiased diagnostic plots of the final model for the entire patient group, some subgroups exhibited slight biases. Firstly, preterm neonates showed a tendency towards higher DVs compared to PRED. The population PK model appeared to overestimate drug clearance in preterm infants, resulting in higher observed carboplatin levels and subsequently a higher observed AUC than predicted. This suggests that the final model did not accurately capture the PK of preterm neonates. Importantly, the observed bias was not related to specific concentrations or sampling times, indicating that it was not influenced by inaccurate recording of sampling time. One possible explanation may be that this BW based final model indeed does not represent the preterm neonates well at all. However, it is noteworthy that the model fit the preterm neonates and infants quite well in all cycles except for cycle 2, suggesting that the observed bias was primarily associated with cycle 2. This indicated that the discrepancy between PRED and DV in preterm neonates was not consistent across all treatment cycles. Therefore, another potential explanation for this observed bias in preterm neonates during cycle 2 is their increased susceptibility to carboplatin-induced nephrotoxicity. It is conceivable that these patients are more susceptible to carboplatin-induced nephrotoxicity, and their renal function may decline more significantly after cycle 1 compared to term infants, leading to impaired clearance and higher drug levels. Considering the existing literature, the hypothesis that preterm neonates are more susceptible to nephrotoxicity in subsequent cycles is plausible, as their renal development is still ongoing and they may exhibit kidney malformations related to nephron prematurity. However, this explanation does not account for the unbiased predictions in cycle 3. It is worth noting that there is limited data on preterm neonates receiving a third cycle of treatment, so the unbiased values in cycle 3 may be a result of chance. One other possible explanation for this is that if toxicity occurs in the

previous cycle, no subsequent cycle is administered. This could potentially introduce selection bias if patients with high drug levels in cycle two experienced toxicity and were excluded from further cycles. Another possibility is that all the observed biases are purely coincidental due to the small number of preterm neonates in the full dataset: only 8 patients. Secondly, a very slight bias was observed in patients with a PNA less than 14 days, with lower DVs than PRED by the population PK model. Chance appears to be the most plausible explanation, given the sparse data in this subgroup. There is no literature-based explanation for this finding either, as one would expect that children in the first days after birth would exhibit reduced clearance compared to what is expected based on their weight, leading to a bias towards higher observed carboplatin values.

This study has several limitations that should be acknowledged. Firstly, the lack of data on the sex of the patients is a notable limitation. Sex differences have been reported to affect the rate of GFR development in neonates and infants, and including this variable as a covariate in our population PK model could have provided valuable insights. Secondly, the validation of the final model could have been more comprehensive. A Normalized Prediction Distribution Errors (NPDE) analysis, which assesses the distribution of prediction errors, was not conducted due to time constraints. This analysis could have provided a more thorough evaluation of the model's performance. Additionally, external validation of the model with other patients was not performed. The 27 excluded patients from the dataset could have been utilized for this purpose, allowing for a more independent assessment of the model's predictive ability. This would have strengthened the robustness and generalizability of the findings. It is important to acknowledge these limitations as they may impact the generalizability and reliability of our conclusions.

In the future, our model could be further validated by conducting a NPDE analysis and by performing external validation using the excluded patients to further validate and assess the performance of the population PK model. Moreover, improving the dataset by including a larger number of preterm infants and those with a PNA of less than 14 days would allow for a more thorough investigation of these specific subgroups. This would enhance the model's ability to capture the unique PK characteristics of these populations and provide more precise dosing recommendations. It is important to

emphasize that any research conducted in this field should always strive to reflect the patient population as it is encountered in the clinical setting. This ensures that the findings and recommendations are applicable and relevant to real-world scenarios. In a broader context, further research into the development of renal function in neonates and young infants would have significant value, not only for optimizing carboplatin dosing but also for dosing regimens of other renally cleared drugs. The ongoing research by Wu et al. holds great potential in this regard. If accurate estimation of renal function continues to pose challenges, exploring alternative biomarkers for assessing renal function in this population would also be recommended. It is also recommended to conduct research with pharmacodynamic (PD) outcomes. This research should specifically focus on evaluating the efficacy and toxicity of carboplatin in neonates and young infants at different target AUC levels. By investigating these aspects, a better understanding of the relationship between drug exposure and desired therapeutic effects, as well as potential adverse reactions, can be gained. Overall, continued research and improvement in this field will contribute to safer and more effective pharmacotherapy for neonates and young infants, ultimately improving patient outcomes.

## **Conclusions**

In conclusion, this study has provided valuable insights into the population PK of carboplatin in neonates and young infants. BW was identified as the most important covariate in the developed two-compartment population PK model. Based on simulations, the optimal daily dose for carboplatin in this population was estimated to be in the range of 5.5-5.8 mg/kg BW. Now that we have gained a better understanding of the intricate PK of carboplatin in neonates and young infants, we can consider adjusting the initial dose to 5.6 mg/kg BW while still employing TDM. The subsequent step would be to gradually phase out TDM in the term infants group. This approach is of utmost importance as it enables us to lessen the dependency on TDM, taking into account the burden imposed on patients due to the need for substantial blood volume collection. However, it should be noted that the model did possibly not adequately capture the PK of preterm neonates, suggesting the need for further TDM and investigation and refinement of the model to better account for this specific population. Also, this research underlines the

importance of continued research in this field to enhance dosing strategies and improve patient outcomes. Further studies, including investigating the PD, as well as validation and refinement of the population PK model

and exploring additional covariates and biomarkers, will be instrumental in optimizing carboplatin therapy in this vulnerable population.

## References

Allen, S., Wilson, M. W., Watkins, A., Billups, C., Qaddoumi, I., Haik, B. H., & Rodriguez-Galindo, C. (2010). Comparison of two methods for carboplatin dosing in children with retinoblastoma. *Pediatric Blood & Cancer*, *55*(1), 47-54. doi:10.1002/pbc.22467

Barnett, S., Kong, J., Makin, G., & Veal, G. J. (2021). Over a decade of experience with carboplatin therapeutic drug monitoring in a childhood cancer setting in the united kingdom. *British Journal of Clinical Pharmacology*, *87*(2), 256-262. doi:10.1111/bcp.14419

De Cock, R. F. W., Allegaert, K., Schreuder, M. F., Sherwin, C. M. T., de Hoog, M., van den Anker, J. N., . . . Knibbe, C. A. J. (2012). Maturation of the glomerular filtration rate in neonates, as reflected by amikacin clearance. *Clinical Pharmacokinetics*, *51*(2), 105-117. doi:10.2165/11595640-000000000-00000

Guignard, J. (2017). 103 - postnatal development of glomerular filtration rate in neonates. In R. A. Polin, S. H. Abman, D. H. Rowitch, W. E. Benitz & W. W. Fox (Eds.), *Fetal and neonatal physiology (fifth edition)* (pp. 993-1002.e2) Elsevier. doi:10.1016/B978-0-323-35214-7.00103-7

Jodrell, D. I., Egorin, M. J., Canetta, R. M., Langenberg, P., Goldbloom, E. P., Burroughs, J. N., . . . Wiltshaw, E. (1992). Relationships between carboplatin exposure and tumor response and toxicity in patients with ovarian cancer. *Jco*, *10*(4), 520-528. doi:10.1200/JCO.1992.10.4.520

Newell, D. R., Pearson, A. D., Balmano, K., Price, L., Wyllie, R. A., Keir, M., . . . Stevens, M. C. (1993). Carboplatin pharmacokinetics in children: The development of a pediatric dosing formula. the united kingdom children's cancer study group. *Jco*, *11*(12), 2314-2323. doi:10.1200/JCO.1993.11.12.2314

Nijstad, A. L., Barnett, S., Lalmohamed, A., Béréanos, I. M., Parke, E., Carruthers, V., . . . Veal, G. J. (2022). Clinical pharmacology of cytotoxic drugs in neonates and infants: Providing evidence-based dosing guidance.

*European Journal of Cancer*, *164*, 137-154. doi:10.1016/j.ejca.2021.11.001

Roberts, E., Mogg, J. A. W., Barnfield, M., & Veal, G. J. (2020). Investigating current practices in renal function measurement and carboplatin dosing in children with cancer – a UK perspective. *Pediatric Hematology and Oncology*, *37*(3), 235-244. doi:10.1080/08880018.2020.1713939

Rodieux, F., Wilboux, M., van den Anker, J. N., & Pfister, M. (2015). Effect of kidney function on drug kinetics and dosing in neonates, infants, and children. *Clinical Pharmacokinetics*, *54*(12), 1183-1204. doi:10.1007/s40262-015-0298-7

Veal, G. J., & Boddy, A. V. (2012). Chemotherapy in newborns and preterm babies. *Seminars in Fetal and Neonatal Medicine*, *17*(4), 243-248. doi:10.1016/j.siny.2012.03.002

Veal, G. J., Cole, M., Errington, J., Pearson, A. D. J., Gerrard, M., Whyman, G., . . . Boddy, A. V. (2010). Pharmacokinetics of carboplatin and etoposide in infant neuroblastoma patients. *Cancer Chemotherapy and Pharmacology*, *65*(6), 1057-1066. doi:10.1007/s00280-009-1111-9

Veal, G. J., Errington, J., Hayden, J., Hobin, D., Murphy, D., Dommett, R. M., . . . Picton, S. (2015). Carboplatin therapeutic monitoring in preterm and full-term neonates. *European Journal of Cancer*, *51*(14), 2022-2030. doi:10.1016/j.ejca.2015.07.011

Wu, Y., Allegaert, K., Flint, R. B., Simons, S. H. P., Krekels, E. H. J., Knibbe, C. A. J., & Völler, S. (2022). Prediction of glomerular filtration rate maturation across preterm and term neonates and young infants using inulin as marker. *The AAPS Journal*, *24*(2), 38. doi:10.1208/s12248-022-00688-z

Zhang, C., Xu, C., Gao, X., & Yao, Q. (2022). Platinum-based drugs for cancer therapy and anti-tumor strategies. *Theranostics*, *12*(5), 2115-2132. doi:10.7150/thno.69424